International Journal of Systems Science

ISSN: (Print) (Online) Journal homepage: https://www.tandfonline.com/loi/tsys20

Model-based recurrent neural network for redundancy resolution of manipulator with remote centre of motion constraints

Zhan Li & Shuai Li

To cite this article: Zhan Li & Shuai Li (2022): Model-based recurrent neural network for redundancy resolution of manipulator with remote centre of motion constraints, International Journal of Systems Science, DOI: 10.1080/00207721.2022.2070790

To link to this article: https://doi.org/10.1080/00207721.2022.2070790

Published online: 31 May 2022.

INTERNATIONAL JOURNAL OF SYSTEMS SCIENCE
https://doi.org/10.1080/00207721.2022.2070790

Taylor & Francis
Taylor & Francis Group

Model-based recurrent neural network for redundancy resolution of manipulator with remote centre of motion constraints

Zhan Li[a] and Shuai Li[b]

[a]Computer Science Department, Swansea University, Swansea, UK; [b]College of Engineering, Swansea University, Swansea, UK

ABSTRACT

Redundancy resolution is a critical issue to achieve accurate kinematic control for manipulators. End-effectors of manipulators can track desired paths well with suitable resolved joint variables. In some manipulation applications such as selecting insertion paths to thrill through a set of points, it requires the distal link of a manipulator to translate along such fixed point and then perform manipulation tasks. The point is known as remote centre of motion (RCM) to constrain motion planning and kinematic control of manipulators. Together with its end-effector finishing path tracking tasks, the redundancy resolution of a manipulators has to maintain RCM to produce reliable resolved joint angles. However, current existing redundancy resolution schemes on manipulators based on recurrent neural networks (RNNs) mainly are focusing on unrestricted motion without RCM constraints considered. In this paper, an RNN-based approach is proposed to solve the redundancy resolution issue with RCM constraints, developing a new general dynamic optimisation formulation containing the RCM constraints. Theoretical analysis shows the theoretical derivation and convergence of the proposed RNN for redundancy resolution of manipulators with RCM constraints. Simulation results further demonstrate the efficiency of the proposed method in end-effector path tracking control under RCM constraints based on an industrial redundant manipulator system.

ARTICLE HISTORY
Received 16 July 2021
Accepted 23 April 2022

KEYWORDS
Redundant; motion planning; kinematics

1. Introduction

Nowadays, manipulators are widely appearing in many industrial and service applications (Jin et al., 2018; Z. Li & Huang, 2020; Z. Li et al., 2020; Su et al., 2019). Manipulators can greatly eliminate inevitable labour burdens on workers by doing repetitive and dull jobs which workers would not like to sustain. Manipulators are usually redundant with extra degrees of freedom (DOFs) in joint space, and therefore they can be utilised to fulfil more flexible and complex manipulation tasks with their end-effectors (Yang et al., 2018, 2019).

Generally speaking, redundancy resolution for kinematic control of manipulators is to seek an optimally-resolved joint variable solution as the reference for accurate servo control in the actuation level, which can eventually generate a desired motion for the end effector in the workspace. However, as we may know, when investigating forward kinematics equations of redundant robots, the resultant mapping between a joint space and a Cartesian workspace exhibits strong coupled nonlinearity all the time. To find the suitable solution in the joint space for manipulator control, it is difficult to inversely obtain the general analytical solutions at the joint space level through directly solving such coupled-nonlinear forward kinematics equations. Therefore, to tackle the redundancy resolution problem in the joint space, the original problem is converted into a problem which considers solutions by making use of velocity kinematics equations of manipulators. Some early works found the control solutions directly by solving the pseudoinverse of the Jacobian matrix of a manipulator (Klein & Huang, 1983; Maciejewski, 1991), and such way of processing may increase local instability and even require additional computational costs which were not expected.

To remedy pseudoinverse-based methods for redundancy resolution, by taking advantage of extra DOFs and such inherent redundancy (Chen, Li, Li, et al., 2020; Z. Li et al., 2020; Su, Qi, et al., 2020), Optimisation-based (e.g. constrained quadratic programming) methods

CONTACT Zhan Li zhan.li@swansea.ac.uk

have been proposed to search for the optimal redundancy resolutions (Chen & Zhang, 2017; Chen et al., 2018; Kanoun et al., 2011; Khan et al., 2020; Ma, 1996; Xu et al., 2019; Z. Zhang et al., 2020). Such optimisation-based methods can involve physical constraints or other types of constraints which can reflect performance indices in motion control (Maciejewski, 1991; Y. Zhang, Chen, et al., 2018; Zhang et al., 2019), but reliable solutions to such constrained optimisation problems cannot be obtained in an analytical manner as well. Some numerical methods in a serial-processing manner have been applied, but they still result in a rather less efficient computational capability. To remedy such shortcomings, dynamic recurrent neural networks (RNNs) with parallel processing ability have been proposed for redundancy resolution and kinematic control with physical constraints (He et al., 2021; S. Li, He, et al., 2017; S. Li et al., 2018, 2019; S. Li, Zhang, et al., 2017; Z. Li et al., 2016; Liao et al., 2016; Z. Zhang et al., 2015; Z. Zhou et al., 2019). For example, in Y. Zhang et al. (2003), joint velocity limits are considered for redundancy resolution synthesised by a dual neural network. In Y. Zhang et al. (2004), a unified quadratic-programming for joint torque optimisation is established by combining the velocity-level and acceleration-level redundancy resolution. In Xiao and Zhang (2013), repetitive motion planning of manipulator with joint acceleration constraints involved is designed. In Guo and Zhang (2014), a minimum-acceleration-norm as the optimisation objective is proposed for obstacle avoidance of manipulators in the joint-acceleration level. In Y. Zhang et al. (2020), redundancy resolution of manipulators with the joint velocity constraints is solved by a passivity-based approach from an energy perspective. In Y. Zhang, Li, et al. (2018), both velocity-level and acceleration-level constraints are integrated into the redundant resolution of manipulators. In S. Li et al. (2012), decentralised kinematic control of multiple redundant manipulators for the cooperative tasks was proposed with a set of joint constraints. In Yahya et al. (2014), geometrically bounded singularities and joint limits are promisingly solved for redundancy resolution with the aid of neural networks. In Chen, Li, Wu, et al. (2020), external disturbances are considered as additional constraints are suppressed by Super-twisting neural network method for coordinated motion control of multiple robot manipulators. In Kong et al. (2019), adaptive fuzzy neural networks are developed for constrained coordinated tasks with impendence learning for robots.

Remote centre of motion (RCM) is a remote fixed point with no physical revolute joint around the location (Su et al., 2019). For motion planning and control of end-effector with tele-operated minimally invasive manipulation, RCM usually leaves a sole point for the manipulator performs positioning or/and insertion (Aghakhani et al., 2013; Su, Schmirander, et al., 2020), e.g. minimally invasive surgery into the subject's body through small incisions, industrial implanting with sensors for detecting cracks. Such applications need to impose physical constraints in joint space to guarantee safe motion generation of the end-effector of the manipulator. One conventional way to do this still needs solving pseudoinverse of Jacobian matrices without task-oriented constraints considered. However, such way of processing may neglect taking advantage of extra DoF to satisfy the RCM constraint as manipulators are redundant. To the best of our knowledge, there are few works reported from aspect of RNN for redundancy resolution of manipulator with RCM constraints.

Motivated by the aforementioned points, currently most of redundancy resolution and kinematic control methods based on RNNs mainly focus on dealing with conventional physical constraints such as joint angle, joint angular velocity and joint acceleration limits. In this paper, in the task-oriented level which is especially for minimally invasive manipulation, we are attempting to propose a new dynamic-model-based method for redundancy resolution of manipulators with RCM constraints synthesised by RNN. The contributions of this work are summarised as follows.

(1) To the best of our knowledge, this paper is the first work on RNN of primal dual type proposed for redundancy resolution and kinematic control of manipulators with RCM constraints.
(2) Simulation results on a 8-link planar manipulator and a Kuka industrial manipulator synthesised by the proposed RNN demonstrate the efficiency of the proposed method in redundancy resolution and kinematic control of manipulators with RCM constraints.

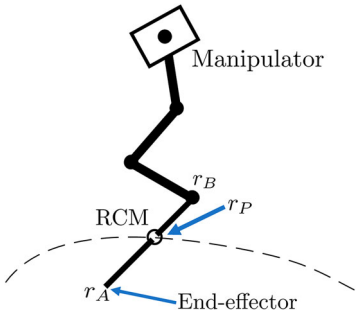

Figure 1. RCM constraint for a redundant manipulator during motion planning and control.

2. Preliminaries

RCM means a remote static/fixed point near the workspace with no physical revolute joint around the location (Aghakhani et al., 2013; Su, Schmirander, et al., 2020). To achieve manipulation such as minimally invasive surgery into the subject's body through small incisions or industrial implanting with sensors for detecting cracks, RCM usually leaves a sole point for the manipulator performs positioning or/and insertion. In addition to the joint physical constraints, RCM imposes an additional constraint on the motion planning and control of redundant manipulator.

Let us consider an n-link manipulator with its end-effector's position is remote from the objective RCM position r_P which is shown in Figure 1, the redundant manipulator executes its task control operations between the two end points r_A and r_B in the workspace. Point r_A is the distal point of the end-effector, point r_B is the distal point of the $n-1$ link. The end-effector of the redundant manipulator has to travel through the objective point r_P along the line/curve between point r_A and point r_B. To describe the motion relation between joints and end-effector, we have

$$\begin{cases} \dot{r}_A = J_1\dot{\theta} \\ \dot{r}_B = J_2\dot{\theta} \end{cases} \tag{1}$$

where $r_A \in R^m$ and $r_B \in R^m$ denote the position vector of the end-effector and the position vector of the end-point of the $n-1$th link of the manipulator respectively, $J_1 \in R^{m\times n}$ and $J_2 \in R^{m\times n}$ respectively denote the Jacobian matrix of the whole manipulator and the Jacobian matrix of the associated $n-1$ link, and $\theta \in R^n$ denotes the joint angle of the manipulator.

In Figure 1, r_P denotes the position vector of the RCM point P, and it can be within the line $A-B$ and the corresponding relation among r_P, r_A and r_B is depicted by

$$r_P - r_B = k(r_A - r_B) \tag{2}$$

where $k \in R$ is a scaling parameter to locate the position r_P with the RCM constraint. Specially, when $k = 0$ is configured statically, then $r_P = r_B$; when $k = 1$ is configured statically, then $r_P = r_A$; when $0 < k < 1$, r_P should be dynamically modulated strictly between points r_A and r_B. The redundancy resolution for kinematic control of the manipulator needs to finish the two tasks: (1) let the end-effector track the desired path accurately and (2) satisfy the RCM constraint to make r_P vary in a very small range or almost static during motion planning and control. In an application scenario, the last link (e.g. $r_A - r_B$) of the manipulator can penetrate a small hole (e.g. r_P) and simultaneously make the end-effector (e.g. r_A) perform the path tracking task.

3. Problem formulation

With a given/resolved joint angle θ, the positions of points r_A and r_B can be determined by directly performing redundancy resolution, but the position of point r_P cannot be determined. Consider r_P is within the line $r_A - r_B$, practically r_P can be described by the introducing a scaling parameter k to associate it with r_A and r_B, thus the state variable pair (θ, k) can describe the redundancy resolution results with RCM constraints. By differentiating the both sides of equation $r_p - r_B = k(r_A - r_B)$ which depicts RCM, one can obtain

$$\dot{r}_P - \dot{r}_B = \dot{k}(r_A - r_B) + k(\dot{r}_A - \dot{r}_B) \tag{3}$$

Then, combining the aforementioned equations (1), we have

$$\dot{r}_P - J_2\dot{\theta} = \dot{k}(r_A - r_B) + k(J_1 - J_2)\dot{\theta} \tag{4}$$

As the point r_P should not move, then r_P should fast converge to a fixed position such as its initial position $r_P(0)$ such that

$$\dot{r}_P = -\varsigma(r_P - r_P(0)), \quad \varsigma \geq 0 \tag{5}$$

where ς is used to scale the convergence of r_P to the initial targeted point $r_P(0)$, guaranteeing the RCM constraint being satisfied during kinematic control process in a timely manner.

As the following equation

$$r_P = k(r_A - r_B) + r_B \tag{6}$$

always holds. Combining the aforementioned equations, next we have

$$\begin{aligned}\varsigma[k(r_A - r_B) + r_B - r_P(0)] + \dot{k}(r_A - r_B)\\ + kJ_1\dot{\theta} + (1-k)J_2\dot{\theta} = 0\end{aligned} \tag{7}$$

i.e.

$$\begin{aligned}\varsigma[k(r_A - r_B) + r_B - r_P(0)] + \dot{k}(r_A - r_B)\\ + [kJ_1 + (1-k)J_2]\dot{\theta} = 0\end{aligned} \tag{8}$$

where we can call the equality above as the RCM constraint for redundancy resolution.

Additionally, to guarantee $k \in [0,1]$ when $k(0) \in [0,1]$, we propose the following inequality constraint for the RCM constraint

$$-c_1 k \le \dot{k} \le -c_1(k-1)$$

where $c_1 > 0$ denotes the scaling parameter to adjust the variation range of k to preserve safety margins.

Based on the derivations and discussions above, we propose the quadratic programming formulation for redundancy resolution of manipulators with RCM constraints as follows:

$$\arg\min_{\theta,k} \quad \dot{\theta}^T\dot{\theta}/2 + c_2\dot{k}^2/2$$

$$\text{s.t.} \quad \begin{cases} \varsigma[k(r_A - r_B) + r_B - r_P(0)] + \dot{k}(r_A - r_B) \\ +[kJ_1 + (1-k)J_2]\dot{\theta} = 0 \\ -c_1 k \le \dot{k} \le -c_1(k-1) \\ \dot{\theta}^- \le \dot{\theta} \le \dot{\theta}^+ \\ J_1\dot{\theta} = -c_3(r_A - r_d) + \dot{r}_d \end{cases} \tag{9}$$

where $c_2 > 0$ denotes one scaling parameter involved in the objective function which shows the joint-velocity based control and RCM constraint based control are simultaneously planned, $c_3 > 0$ denotes the parameter to scale convergence for the end-effector position tracking, r_d denotes the desired position vector for the end-effector to track, and $\dot{\theta}^-$ and $\dot{\theta}^+$ are the lower and upper joint velocity limits respectively.

In the proposed optimisation formulation for redundancy resolution with RCM constraints, the position of r_P is dynamically adjusted by parameter k with simultaneous positions r_A and r_B. The initial value $k(0)$ is chosen according to the specific scenarios for safe manipulation, e.g. when $t = 0$, r_P can be chosen in the middle of the line $A-B$, and thus $k(0) = 0.5$.

To maintain the RCM constraint, $\dot{\theta}$ and $\dot{k}$ are used as decision variables, and the variable which really controls the manipulator is $\dot{\theta}$ as the control input action. In practice, we can therefore solve $\dot{k}$ and substitute it into the aforementioned proposed optimisation formulation and thus the RCM constraint can be satisfied and modulated by resolving the joint angle variable θ.

The advantages of the proposed method is that the RNN for redundancy resolution with the RCM constraint does not need to know the exact position r_P for the fixed point P, which may save the sensor equipping. For manipulation safety, we can exert more margins like making the variable k under the range/limit $0.3 \le k \le 0.7$ or $0.2 \le k \le 0.8$.

4. Proposed RNN for redundancy resolution with RCM constraints

In this section, the modelling and convergence of the proposed RNN for redundancy resolution with RCM constraints are addressed.

4.1. Model description

To solve redundancy resolution problem with RCM constraints, first, according to the Karush–Kuhn–Tucker (KKT) conditions (Boyd & Vandenberghe, 2004), we need to first define the Lagrange function which is associated with the objective function $\dot{\theta}^T\dot{\theta}/2 + c_2\dot{k}^2/2$, the RCM constraint and the differential kinematics constraint as follows:

$$\begin{aligned}L = \dot{\theta}^T\dot{\theta}/2 + c_2\dot{k}^2/2 + \lambda_1^T[\varsigma(k(r_A - r_B) + r_B - r_p(0))\\ + \dot{k}(r_A - r_B) + kJ_1\dot{\theta} + (1-k)J_2\dot{\theta}]\\ + \lambda_2^T[J_1\dot{\theta} + c_3(r_A - r_d) - \dot{r}_d]\end{aligned} \tag{10}$$

where λ_1 and λ_2 denote the Lagrange multiplier vectors which are respectively associated with the RCM constraint and the differential kinematic constraint. Such definition of Lagrange function different from the one of the well-known Hamiltonian form that appear in an aspect of robotic dynamics derivation. The partial derivatives of the Lagrange function with

respect to $\dot{\theta}$, $\dot{k}$, λ_1 and λ_2 are

$$\begin{cases} \dfrac{\partial L}{\partial \dot{\theta}} = \dot{\theta} + [kJ_1 + (1-k)J_2]^T\lambda_1 + J_1^T\lambda_2 \\ \dfrac{\partial L}{\partial \dot{k}} = c_2\dot{k} + \lambda_1^T(r_A - r_B) \\ \dfrac{\partial L}{\partial \lambda_1} = \varsigma(k(r_A - r_B) + r_B - r_p(0)) \\ \quad +(kJ_1 + (1-k)J_2)\dot{\theta} + \dot{k}(r_A - r_B) \\ \dfrac{\partial L}{\partial \lambda_2} = J_1\dot{\theta} + c_3(r_A - r_d) - \dot{r}_d \end{cases} \tag{11}$$

According to the design principle of the primal dual neural network model for solving constrained optimisation, we thus construct the following RNN solver:

$$\begin{cases} \epsilon_z\dot{z} = -z + P_\Omega\left(z - \dfrac{\partial L}{\partial z}\right) \\ \epsilon_1\dot{\lambda}_1 = \dfrac{\partial L}{\partial \lambda_1} \\ \epsilon_2\dot{\lambda}_2 = \dfrac{\partial L}{\partial \lambda_2} \end{cases} \tag{12}$$

where $z = [\dot{\theta}, \dot{k}]$, $P_\Omega(\cdot)$ denotes the piecewise linear projection function array with the solution set Ω, i.e.

$$P_\Omega(u) = \begin{cases} u^-; u < u^- \\ u; u^- \le u \le u^+ \\ u^+; u > u^+ \end{cases}$$

and $\epsilon_z > 0$, $\epsilon_1 > 0$ and $\epsilon_2 > 0$ are the convergence-scale parameters to accelerate solutions of the RNN solver when increased. By substituting aforementioned partial derivatives equations into the RNN solver, we have the specifical form of the RNN solver for redundancy resolution with RCM constraints

$$\begin{cases} \epsilon_z\dot{z} = P_\Omega\left(z - \begin{bmatrix} \dot{\theta} + (kJ_1 + (1-k)J_2)^T\lambda_1 + J_1^T\lambda_2 \\ c_2\dot{k} + \lambda_1^T(r_A - r_B) \end{bmatrix}\right) \\ \qquad - z \\ \epsilon_1\dot{\lambda}_1 = \varsigma(k(r_A - r_B) + r_B - r_p(0)) \\ \qquad + (kJ_1 + (1-k)J_2)\dot{\theta} + \dot{k}(r_A - r_B) \\ \epsilon_2\dot{\lambda}_2 = J_1\dot{\theta} + c_3(r_A - r_d) - \dot{r}_d \end{cases} \tag{13}$$

where the convergence scaling parameters can be configured as $\epsilon_z = \epsilon_1 = \epsilon_2 = \epsilon > 0$ for unity. Figure 2 shows the architecture of the corresponding RNN for RCM-based kinematic control of manipulator.

4.2. Theoretical analysis

Due to its convexity of the optimisation problem and note that the aforementioned expression $\partial L/\partial z \in \Omega$ includes the normal cone operator on z. Recall the property on the linear projection to a normal cone, the solution of optimisation problem is equivalent to the solution of the piecewise linear projection equations $P_\Omega(\cdot)$. The dynamic optimisation solver based on the primal dual neural network model solves the linear projection equations when the equilibrium point u is reached (Gao, 2003; Gao & Liao, 2003). Therefore, one can define a Lyapunov function $V(z) = z^Tz/2 \ge 0$ and obtain its time derivative $\dot{V} = -z^T[u - P_\Omega(z - \frac{\partial L(z,\lambda)}{\partial z})]/\epsilon \le -z^Tz/\epsilon \le 0$, thus the convergence to the equilibrium point can be achieved. Therefore, $\dot{z} = 0$, $\dot{\lambda}_1 = 0$ and $\dot{\lambda}_2 = 0$ are achieved in the steady state. In this situation, as $\dot{\lambda}_2 = 0$ is held in the steady state, which means $J_1\dot{\theta} + c_3(r_A - r_d) - \dot{r}_d = 0$ is guaranteed, i.e. $\dot{r}_A - \dot{r}_d = c_3(r_A - r_d)$. It indicates that the error between r_A and the reference trajectory r_d can converge to zero finally.

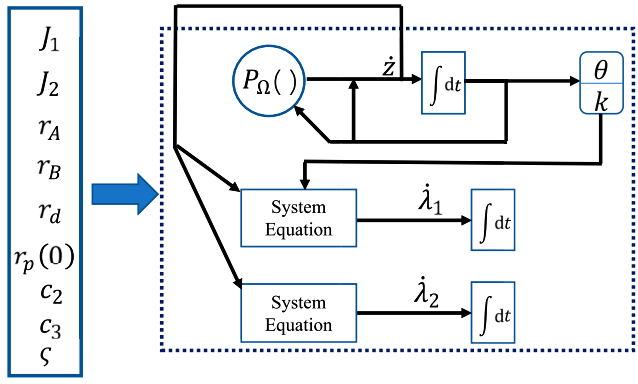

Figure 2. The overall RNN architecture for RCM based kinematic control of manipulator. The RNN of the primal dual type possess its neural states θ, k, λ_1 and λ_2, the inputs of the RNN are: model's differential kinematic information J_1 and J_2, the position information of different links' end-effectors r_A, r_B and r_d, the desired RCM position information $r_p(0)$ and rest parameter information. With these input information, the training process of the RNN will try to minimise to objective function (energy function) with constraints and let the neural network states θ, k, λ_1 and λ_2 converge to their equilibrium points with the convergence/learning rate $\epsilon_z = \epsilon_1 = \epsilon_2$.

5. Simulation results

In this section, simulation results on kinematic control of two kinds of redundant robots are given to validate the proposed method for safe redundancy resolution with RCM constraints. The first one is a 8-link planar robot and the other one is a Kuka 7-DoF robot. The RCM constraint for the 8-link planar robot is locating between the r_A and r_B, where r_A is the position of the

end-effector and r_B is the position of the remote point of its seventh link. The RCM constraint of the Kuka 7-DoF robot is locating between the r_A and r_B, where r_A is the position of the remote point at an additional link from the end-effector and r_B is the position of the end-effector.

5.1. Simulation configuration

In the simulation, we first examine the performance for the 8-link planar robot arm by the proposed method. The lengths of the links are set as $l_1 = 0.2$, $l_2 = 0.15$, $l_3 = 0.15$, $l_4 = 0.15$, $l_5 = 0.15$, $l_6 = 0.15$, $l_7 = 0.15$ and $l_8 = 0.15$ m. The 8-link planar robot arm's kinematics is depicted by

$$T_8(\theta) = T_1(\theta)T_2(\theta)\cdots T_i(\theta)\cdots T_7(\theta)T_8(\theta)$$

where $T_i(\theta)$ denotes the homogeneous transformation matrix between the adjacent joints of the 8-link planar robot arm. According to such configuration, the 8-link planar robot arm's Jacobian matrix for such 8-link planar robot arm is obtained by

$$J = \begin{bmatrix} \frac{\mathrm{d}r_y}{\mathrm{d}\theta_1} & \frac{\mathrm{d}r_y}{\mathrm{d}\theta_2} & \cdots & \frac{\mathrm{d}r_y}{\mathrm{d}\theta_n} \\ \frac{\mathrm{d}r_z}{\mathrm{d}\theta_1} & \frac{\mathrm{d}r_z}{\mathrm{d}\theta_2} & \cdots & \frac{\mathrm{d}r_z}{\mathrm{d}\theta_n} \end{bmatrix} \in R^{2\times 8}$$

where

$$\begin{cases} \frac{\mathrm{d}r_y}{\mathrm{d}\theta_1} = -\sum_{i=1}^{8} l_i s_i \\ \frac{\mathrm{d}r_y}{\mathrm{d}\theta_2} = -\sum_{i=2}^{8} l_i s_i \\ \vdots \\ \frac{\mathrm{d}r_y}{\mathrm{d}\theta_8} = -l_8 s_8 \end{cases} \quad \text{and} \quad \begin{cases} \frac{\mathrm{d}r_z}{\mathrm{d}\theta_1} = \sum_{i=1}^{8} l_i c_i \\ \frac{\mathrm{d}r_z}{\mathrm{d}\theta_2} = \sum_{i=2}^{8} l_i c_i \\ \vdots \\ \frac{\mathrm{d}r_z}{\mathrm{d}\theta_8} = l_8 c_8 \end{cases}$$

with

$$s_i = \sin(\theta_1 + \theta_2 + \cdots + \theta_i)$$

and

$$c_i = \cos(\theta_1 + \theta_2 + \cdots + \theta_i)$$

The desired paths are planned as a circle with its radius being 0.05 m and a square with its length being 0.06 m. The convergence parameter ϵ of the primal dual neural network solver for the proposed method is chosen as 0.0001, the initial value of k is set as 0.4, parameters $\varsigma = 10$, $c_2 = 1$ and $c_3 = 10$ are configured.

Table 1. D-H parameters of the Kuka manipulator.

Link	a_i (m)	α_i (rad)	d_i (m)
1	0	$-\pi/2$	0.340
2	0	$\pi/2$	0
3	0	$\pi/2$	0.400
4	0	$-\pi/2$	0
5	0	$-\pi/2$	0.400
6	0	$\pi/2$	0
7	0	0	0.126

Next, the performance of the proposed method on the Kuka redundant robot is examined. The D–H parameter is according to Table 1 (Z. Li et al., 2020). The desired paths are planned as follows : (i) a circle with its radius being 0.15 m, (ii) a square with its length being 0.20 m, (iii) a tetracuspid curve with its mathematical form being $r_d = [0.15\cos^3\omega t, 0.15\sin^3\omega t, 0]^{\mathrm{T}}$ with $\omega = 0.5$ and (iv) a '8' shape (eight-character) curve with its mathematical form being $r_d = [0.16\cos\omega_1 t, 0.15\sin\omega_2 t, 0]^{\mathrm{T}}$ with $\omega_1 = 0.5$ and $\omega_2 = 0.8$. The convergence parameter ϵ of the primal dual neural network solvers for the proposed method is chosen as 0.0001, the initial value of k is set as 0.4, parameters $\varsigma = 10$, $c_2 = 1$ and $c_3 = 10$ are configured.

5.2. Performance of 8-link planar robot arm

Figure 3 presents the comprehensive performance of the proposed method on the 8-link planar robot arm for circle path tracking. Figure 3(a) shows the circle path tracking process, and we can roughly observe that the path tracking is well done with RCM constraint satisfied (a point r_P is obviously seen). Figure 3(b) shows the position error $[E_x, E_y]$ of the end-effector, and we can evidently see that the position error $[E_x, E_y]$ fast converges to zero. Figure 3(c) shows resolved joint angle for the 8-link planar robot by the proposed method. Figure 3(d) shows the 2D coordinates of the r_P point, and we see that its X-axis coordinate r_{px} is changing from -0.02 to -0.005 m and its Y-axis coordinate r_{px} is changing from 0.523 to 0.53 m. The r_P point is changing in a very small range in both X-axis and Y-axis, which is much less as compared with the radius of the circle path to track. Figure 3(e) shows convergence of the variable k which is used to maintain the motion planning constrained by RCM. Figure 3(f) further shows the convergence of the r_P point, and it can be seen that point r_P can fast converge to the steady state which makes it static after the transient process.

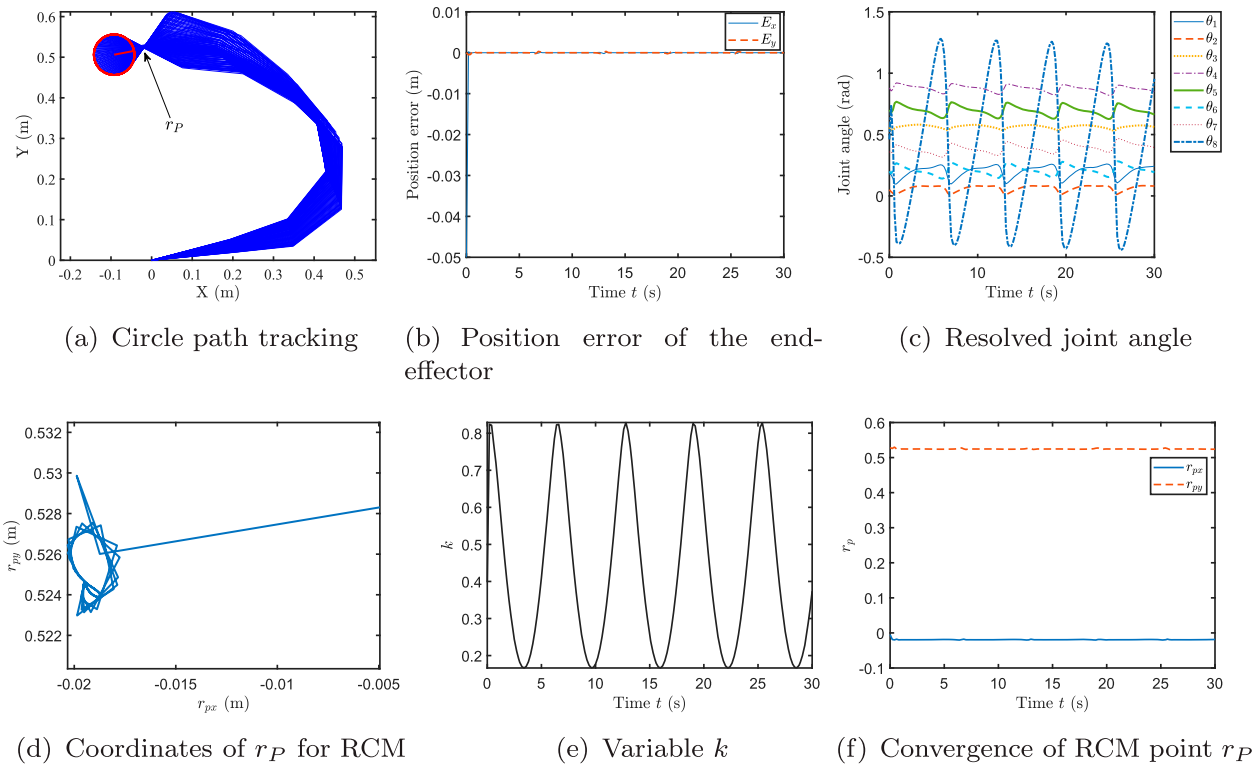

(a) Circle path tracking (b) Position error of the end-effector (c) Resolved joint angle

(d) Coordinates of r_P for RCM (e) Variable k (f) Convergence of RCM point r_P

Figure 3. Comprehensive performance of the proposed method for circle path tracking with the RCM constraint for the 8-link planar manipulator. The RCM point is kept non-stationary while the circle path tracking task for the end-effector is performed simultaneously. One could observe that the position error of the end-effector converges to zero and the 2D RCM coordinates are held in the steady-state: (a) circle path tracking, (b) position error of the end-effector, (c) resolved joint angle, (d) coordinates of r_P for RCM, (e) variable k and (f) convergence of RCM point r_P.

All these results verify the proposed method is efficient for the 8-link planar robot on kinematic control with the RCM constraint.

Figure 4 presents the comprehensive performance of the proposed method on the 8-link planar robot arm for square path tracking. Figure 4(a) shows the square path tracking process, and we can roughly observe that the path tracking is well done with RCM constraint satisfied (a point r_P is obviously seen). Figure 4(b) shows the position error $[E_x, E_y]$ of the end-effector, and we can evidently see that the position error $[E_x, E_y]$ fast converges to zero. Figure 4(c) shows resolved joint angle for the 8-link planar robot by the proposed method. Figure 4(d) shows the 3D coordinates of the r_P point, and we see that its coordinate r_p is changing from -0.02 to -0.005 m and its Y-axis coordinate r_{px} is changing from 0.523 to 0.53 m. The r_P point is changing in a very small range in both X-axis and Y-axis, which is much less as compared with the radius of the circle path to track. Figure 4(e) shows the convergence of the variable k which is used to maintain the motion planning constrained by RCM. Figure 4(f) further shows the convergence of the r_P point, and it can be seen that point r_P can fast converge to the steady state which makes it static after the transient process. All these results verify the proposed method is efficient for the 8-link planar robot on kinematic control with the RCM constraint.

5.3. Performance of 7-DoF redundant robot

Figure 5 presents the comprehensive performance of the proposed method on the Kuka redundant robot arm for circle path tracking. Figure 5(a) shows the circle path tracking process, and we can roughly observe that the path tracking is well done with RCM constraint satisfied (a point r_P is obviously seen). Figure 5(b) shows the position error $[E_x, E_y, E_z]$ of the end-effector, and we can evidently see that the position error $[E_x, E_y, E_z]$ fast converges to zero. Figure 5(c) shows resolved joint angle for the 8-link planar robot by the proposed method. Figure 5(d) shows the 3D

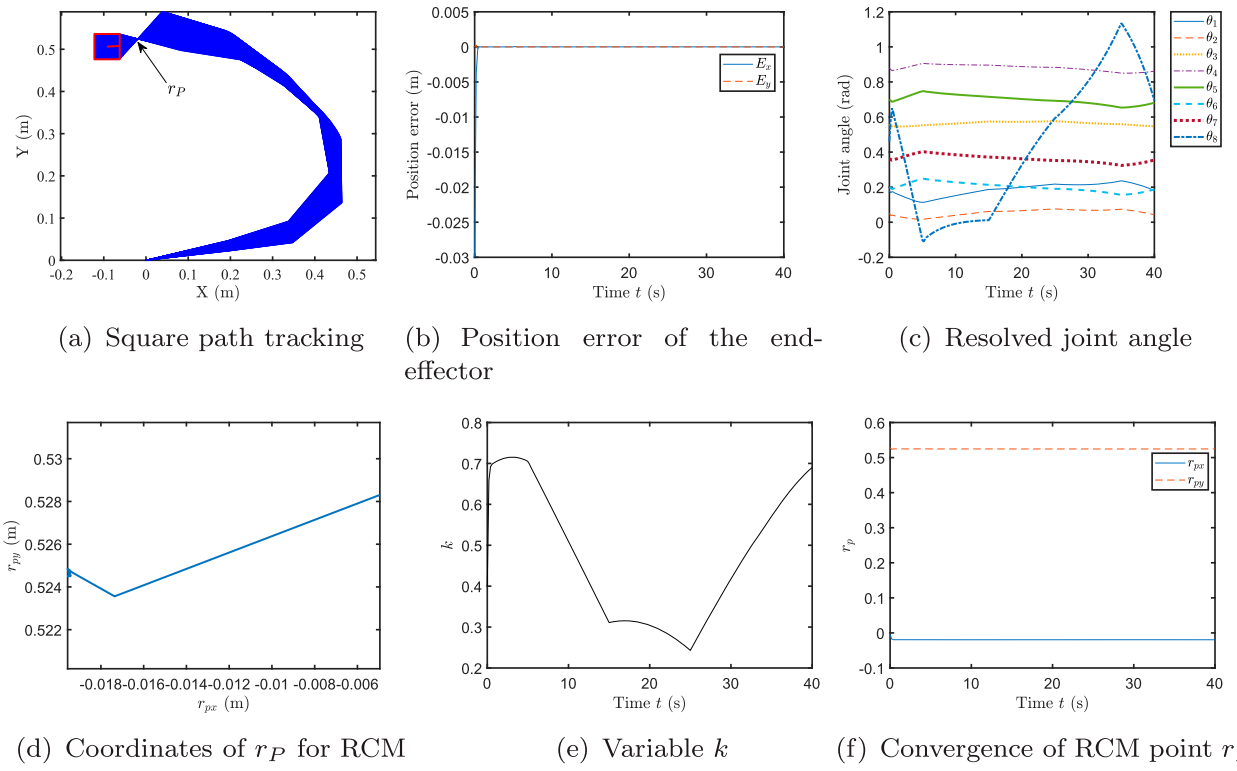

(a) Square path tracking (b) Position error of the end-effector (c) Resolved joint angle

(d) Coordinates of r_P for RCM (e) Variable k (f) Convergence of RCM point r_P

Figure 4. Comprehensive performance of the proposed method for square path tracking with the RCM constraint for the 8-link planar manipulator. The RCM point is kept non-stationary while the square path tracking task for the end-effector is performed simultaneously. One could observe that the position error of the end-effector converges to zero and the 2D RCM coordinates are held in the steady-state. (a) Square path tracking, (b) position error of the end-effector, (c) resolved joint angle, (d) coordinates of r_P for RCM, (e) variable k and (f) convergence of RCM point r_P.

coordinates of the r_P point, and we see that its 3D coordinate r_p is with a very small range and almost static. The r_P point is changing in a very small range and is much less as compared with the radius of the circle path to track. Figure 5(e) shows the convergence of the variable k which is used to maintain the motion planning constrained by RCM. Figure 5(f) further shows the convergence of the r_P point, and it can be seen that point r_P can fast converge to the steady state which makes it static after the transient process. All these results verify the proposed method is efficient for the Kuka redundant robot arm on circle path tracking control with the RCM constraint satisfied.

Figure 6 presents the comprehensive performance of the proposed method on the Kuka redundant robot arm for square path tracking. Figure 6(a) shows the square path tracking process, and we can roughly observe that, the path tracking is well done with RCM constraint satisfied (a point r_P is obviously seen). Figure 6(b) shows the position error $[E_x, E_y, E_z]$ of the end-effector, and we can evidently see that the position error $[E_x, E_y, E_z]$ fast converges to zero. Figure 6(c) shows resolved joint angle for the 8-link planar robot by the proposed method. Figure 5(d) shows the 2D coordinates of the r_P point, and we see that its 3D coordinate r_p is changing in a very small range and almost fixed. The r_P point is changing in a very small range and is much less as compared with the length of the square path to track. Figure 6(e) shows the convergence of the variable k which is used to maintain the motion planning constrained by RCM. Figure 6(f) further shows the convergence of the r_P point, and it can be seen that point r_P can fast converge to the steady state which makes it static after the transient process. All these results verify the proposed method is efficient for the Kuka redundant robot arm on square path tracking control with the RCM constraint satisfied.

Figure 7 presents the comprehensive performance of the proposed method on the Kuka redundant robot arm for tetracuspid path tracking. Figure 7(a) shows the tetracuspid path tracking process, and we can roughly observe that, the path tracking is well done

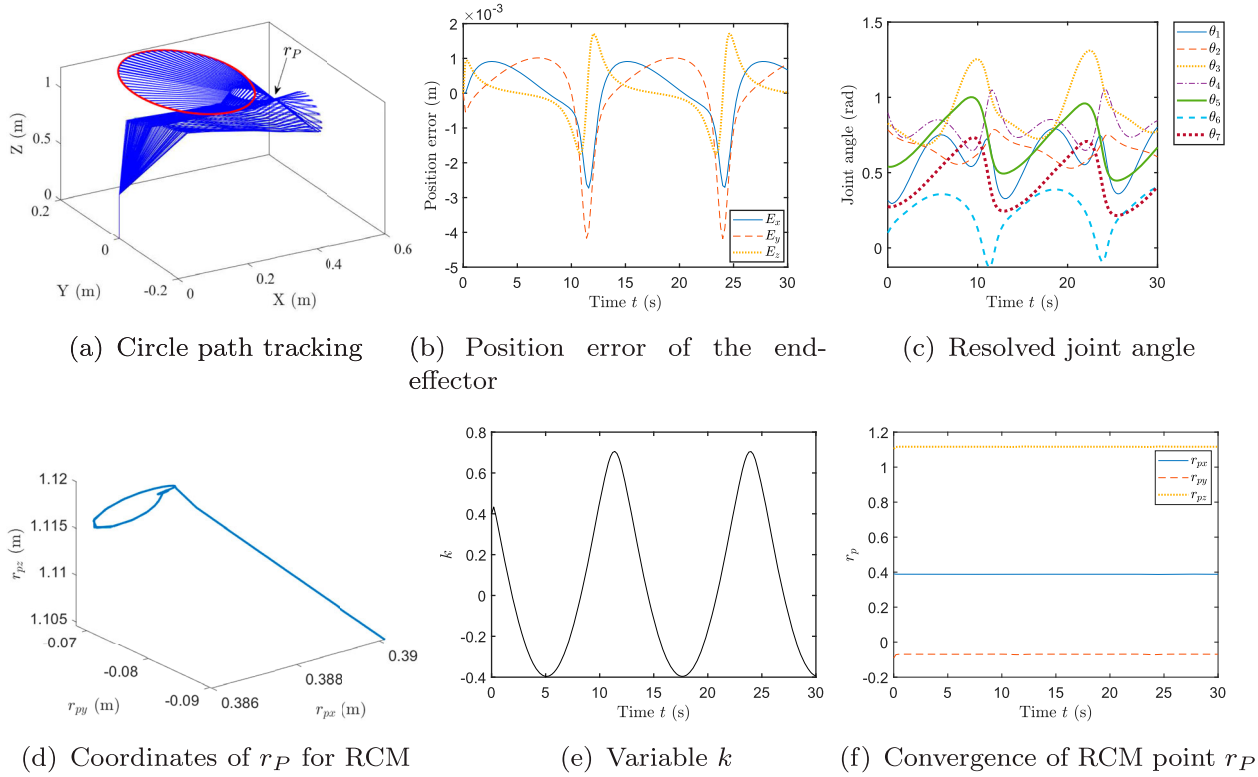

(a) Circle path tracking (b) Position error of the end-effector (c) Resolved joint angle

(d) Coordinates of r_P for RCM (e) Variable k (f) Convergence of RCM point r_P

Figure 5. Comprehensive performance of the proposed method for circle path tracking with the RCM constraint for the Kuka manipulator. The RCM point is kept non-stationary while the circle path tracking task for the end-effector is performed simultaneously. One could observe that the position error of the end-effector converges to zero and the 3D RCM coordinates are held in the steady-state: (a) circle path tracking, (b) position error of the end-effector, (c) resolved joint angle, (d) coordinates of r_P for RCM, (e) variable k and (f) convergence of RCM point r_P.

with RCM constraint satisfied (a point r_P is obviously seen). Figure 7(b) shows the position error $[E_x, E_y, E_z]$ of the end-effector, and we can evidently see that the position error $[E_x, E_y, E_z]$ fast converges to zero. Figure 7(c) shows resolved joint angle for the redundant robot arm by the proposed method. Figure 7(d) shows the 3D coordinates of the r_P point, and we see that its 3D r_p is almost fixed with very small position changes. Figure 6(e) shows the convergence of the variable k which is used to maintain the motion planning constrained by RCM. Figure 7(f) further shows the convergence of the r_P point, and it can be seen that point r_P can fast converge to the steady state which makes it static after the transient process. All these results verify the proposed method is efficient for the Kuka redundant robot arm on tetracuspid path tracking control with the RCM constraint satisfied.

Figure 8 further presents the comprehensive performance of the proposed method on the Kuka redundant robot arm for 'eight-character' path tracking. Figure 8(a) shows the 'eight-character' path tracking process, and we can roughly observe that, the path tracking is well done with RCM constraint satisfied (a point r_P is obviously seen). Figure 8(b) shows the position error $[E_x, E_y, E_z]$ of the end-effector, and we can evidently see that the position error $[E_x, E_y, E_z]$ fast converges to zero. Figure 8(c) shows resolved joint angle for the 8-link planar robot by the proposed method. Figure 8(d) shows the 3D coordinates of the r_P point, which is almost fixed with very small position changes. Figure 8(e) shows convergence of the variable k which is used to maintain the motion planning constrained by RCM. Figure 8(f) further shows the convergence of the r_P point, and it can be seen that point r_P can fast converge to the steady state which makes it static after the transient process. All these results verify the proposed method is efficient for the Kuka redundant robot arm on 'eight-character' path tracking control with the RCM constraint satisfied.

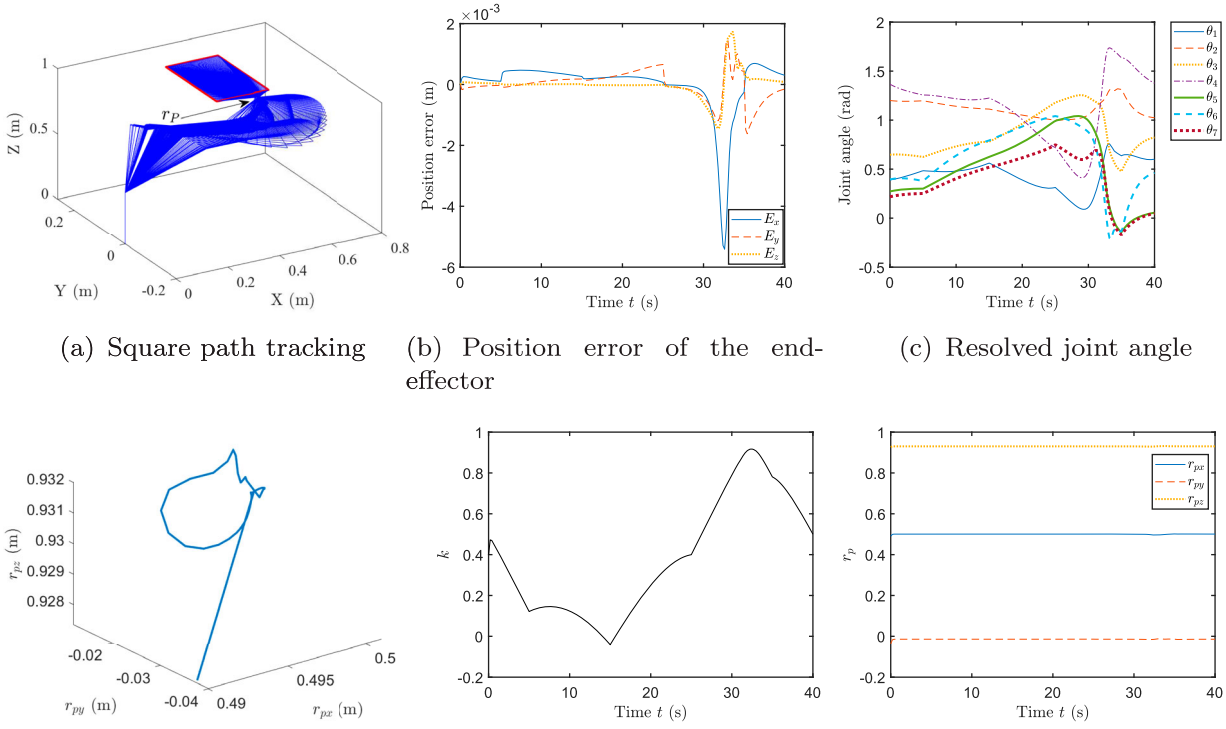

(a) Square path tracking (b) Position error of the end-effector (c) Resolved joint angle

(d) Coordinates of r_P for RCM (e) Variable k (f) Convergence of RCM point r_P

Figure 6. Comprehensive performance of the proposed method for square path tracking with the RCM constraint for the Kuka manipulator. The RCM point is kept non-stationary while the square path tracking task for the end-effector is performed simultaneously. One could observe that the position error of the end-effector converges to zero and the 3D RCM coordinates are held in the steady-state. (a) Square path tracking, (b) position error of the end-effector, (c) resolved joint angle, (d) coordinates of r_P for RCM, (e) variable k and (f) convergence of RCM point r_P.

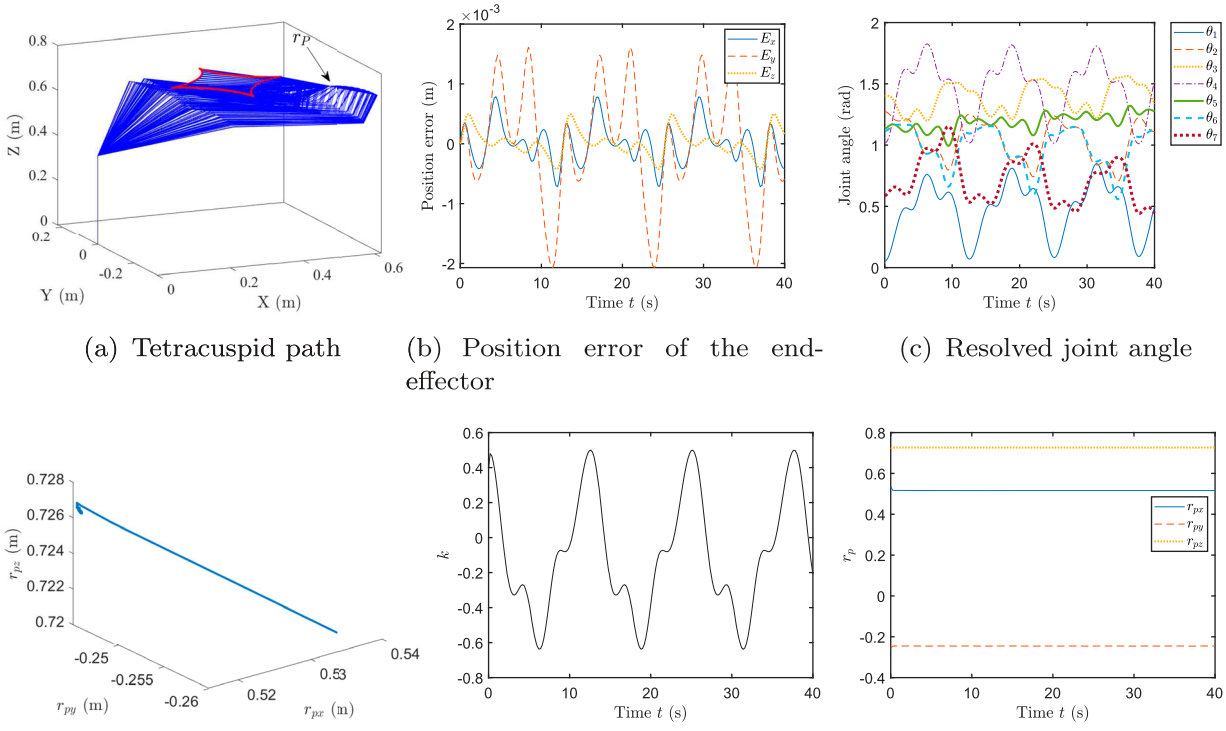

(a) Tetracuspid path (b) Position error of the end-effector (c) Resolved joint angle

(d) Coordinates of r_P for RCM (e) Variable k (f) Convergence of RCM point r_P

Figure 7. Comprehensive performance of the proposed method for tetracuspid path tracking with the RCM constraint for the Kuka manipulator: (a) tetracuspid path, (b) position error of the end-effector, (c) resolved joint angle, (d) coordinates of r_P for RCM, (e) variable k and (f) convergence of RCM point r_P.

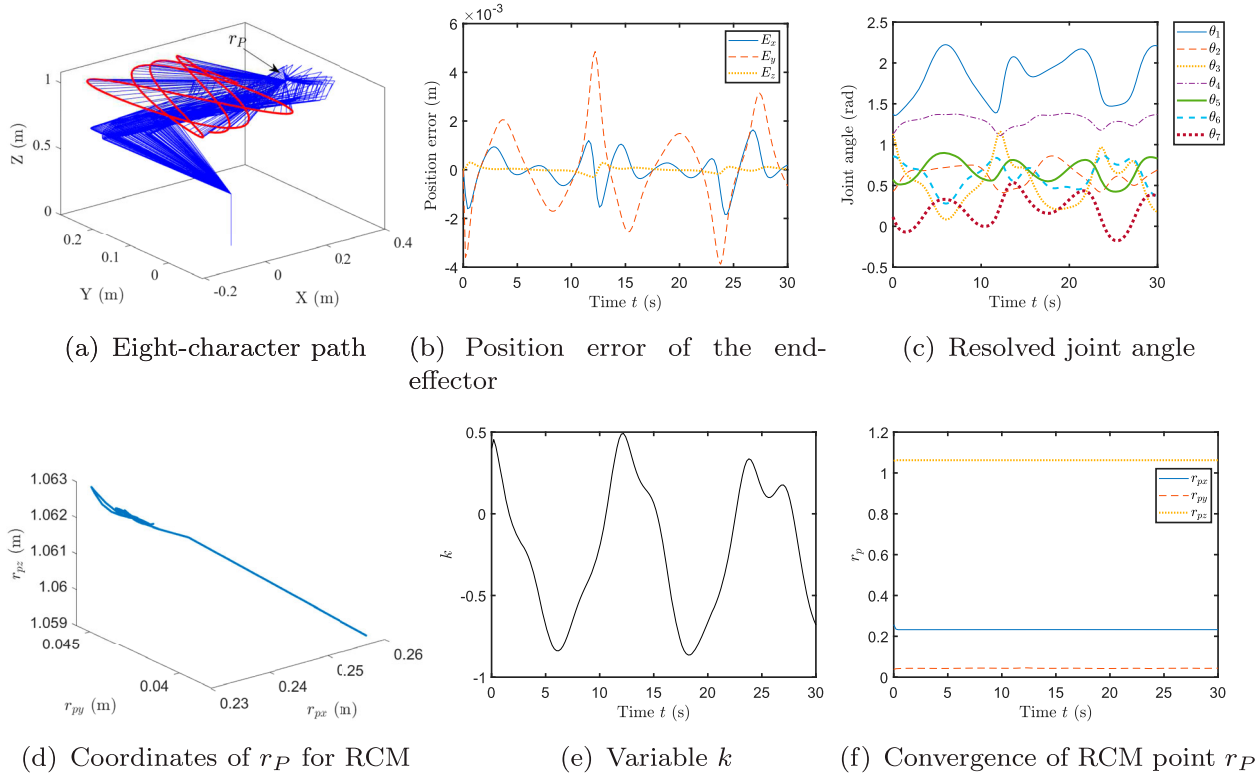

(a) Eight-character path (b) Position error of the end-effector (c) Resolved joint angle

(d) Coordinates of r_P for RCM (e) Variable k (f) Convergence of RCM point r_P

Figure 8. Comprehensive performance of the proposed method for eight-character path tracking with the RCM constraint for the Kuka manipulator: (a) eight-character path, (b) position error of the end-effector, (c) resolved joint angle, (d) coordinates of r_P for RCM, (e) variable k and (f) convergence of RCM point r_P.

To summarise, the proposed RNN-based method is efficient for redundancy resolution of manipulators with RCM constraints. The proposed method can guarantee the convergence of the optimal solution for the resolved joint angle $\dot{\theta}$ and RCM modulation variable k simultaneously, and the position of the point r_P for RCM can be modulated in a very small range and almost static in space.

6. Conclusion

Current existing redundancy resolution schemes on manipulators based on RNNs mainly focusing on unrestricted motion without RCM constraints. In this paper, for the first time, a recurrent neural network is proposed to solve the redundancy resolution issue with RCM constraints, with a new and general dynamic optimisation formulation containing the RCM constraints. Theoretical analysis shows the derivation and convergence of the proposed RNN for redundancy resolution of manipulators with RCM constraints. Simulation results further demonstrate the efficiency of the proposed method in end-effector path tracking control under RCM constraints based on an industrial redundant manipulator system. The limitations of the study might include that redundant manipulators have to obligate enough extra DoFs to satisfy both RCM constraints and physical constraints. Future works can be directed into data-driven based learning control approaches synthesised by discrete-time version of RNN.

Data availability statement

The codes and data that support the this study are available on request from the corresponding author Zhan Li. The data are not publicly available due to copyright restrictions by the authors on potential applications in robotics.

Disclosure statement

No potential conflict of interest was reported by the author(s).

Notes on contributors

Zhan Li received the B.S. and M.S. degrees from Sun Yat-sen University, Guangzhou, China, in 2009 and 2011, respectively, and the Ph.D. degree from INRIA and University of Montpellier, Montpellier, France, in 2014. He is currently a Senior Lecturer with the Department of Computer Science, Swansea University, Swansea, U.K. His current research interests include intelligent control of medical/service robotics and biosignal processing. Dr. Li serves as an Editorial Board Member for *PLOS One* and a Guest Editor for *Frontiers in Neurorobotics* and *Frontiers in Neuroscience*.

Shuai Li received the B.E. degree in precision mechanical engineering from Hefei University of Technology, Hefei, China, in 2005, the M.E. degree in automatic control engineering from the University of Science and Technology of China, Hefei, in 2008, and the Ph.D. degree in electrical and computer engineering from Stevens Institute of Technology, Hoboken, NJ, USA, in 2014. He is currently an Associate Professor (Reader) at Swansea University, Swansea, U.K., leading the Robotic Laboratory, conducting research on robot manipulation and impedance control, multi-robot coordination, distributed control, intelligent optimization and control, and legged robots. Dr. Li was the General Co-Chair of *2018 International Conference on Advanced Robotics and Intelligent Control*. He is the Founding Editor-in-Chief of *International Journal of Robotics and Control*.

References

Aghakhani, N., Geravand, M., Shahriari, N., Vendittelli, M., & Oriolo, G. (2013). Task control with remote center of motion constraint for minimally invasive robotic surgery. In *2013 IEEE international conference on robotics and automation* (pp. 5807–5812). IEEE.

Boyd, S., & Vandenberghe, L. (2004). *Convex optimization*. Cambridge University Press.

Chen, D., Li, S., Li, W., & Wu, Q. (2020). A multi-level simultaneous minimization scheme applied to jerk-bounded redundant robot manipulators. *IEEE Transactions on Automation Science and Engineering*, *17*(1), 463–474. https://doi.org/10.1109/TASE.8856

Chen, D., Li, S., Wu, Q., & Luo, X. (2020). Super-twisting ZNN for coordinated motion control of multiple robot manipulators with external disturbances suppression. *Neurocomputing*, *371*(3), 78–90. https://doi.org/10.1016/j.neucom.2019.08.085

Chen, D., & Zhang, Y. (2017). A hybrid multi-objective scheme applied to redundant robot manipulators. *IEEE Transactions on Automation Science and Engineering*, *14*(3), 1337–1350. https://doi.org/10.1109/TASE.2015.2474157

Chen, D., Zhang, Y., & Li, S. (2018). Zeroing neural-dynamics approach and its robust and rapid solution for parallel robot manipulators against superposition of multiple disturbances. *Neurocomputing*, *275*(6), 845–858. https://doi.org/10.1016/j.neucom.2017.09.032

Gao, X.-B. (2003, March). Exponential stability of globally projected dynamic systems. *IEEE Transactions on Neural Networks*, *14*(2), 426–431. https://doi.org/10.1109/TNN.2003.809409

Gao, X.-B., & Liao, L.-Z. (2003). A neural network for monotone variational inequalities with linear constraints. *Physics Letters A*, *307*(2–3), 118–128. https://doi.org/10.1016/S0375-9601(02)01673-0

Guo, D., & Zhang, Y. (2014). Acceleration-level inequality-based man scheme for obstacle avoidance of redundant robot manipulators. *IEEE Transactions on Industrial Electronics*, *61*(12), 6903–6914. https://doi.org/10.1109/TIE.2014.2331036

He, W., Mu, X., Zhang, L., & Zou, Y. (2021). Modeling and trajectory tracking control for flapping-wing micro aerial vehicles. *IEEE/CAA Journal of Automatica Sinica*, *8*(1), 148–156. https://doi.org/10.1109/JAS.2020.1003417

Jin, L., Li, S., Yu, J., & He, J. (2018). Robot manipulator control using neural networks: A survey. *Neurocomputing*, *285*(2), 23–34. https://doi.org/10.1016/j.neucom.2018.01.002

Kanoun, O., Lamiraux, F., & Wieber, P. (2011). Kinematic control of redundant manipulators: Generalizing the task-priority framework to inequality task. *IEEE Transactions on Robotics*, *27*(4), 785–792. https://doi.org/10.1109/TRO.2011.2142450

Khan, A. H., Li, S., Chen, D., & Liao, L. (2020). Tracking control of redundant mobile manipulator: An RNN based metaheuristic approach. *Neurocomputing*, *400*(11), 272–284. https://doi.org/10.1016/j.neucom.2020.02.109

Klein, C. A., & Huang, C. H. (1983). Review of pseudoinverse control for use with kinematically redundant manipulators. *IEEE Transactions on Systems, Man, and Cybernetics*, *SMC-13*(2), 245–250. https://doi.org/10.1109/TSMC.1983.6313123

Kong, L., He, W., Yang, C., Li, Z., & Sun, C. (2019). Adaptive fuzzy control for coordinated multiple robots with constraint using impedance learning. *IEEE Transactions on Cybernetics*, *49*(8), 3052–3063. https://doi.org/10.1109/TCYB.2018.2838573

Li, S., Chen, S., Liu, B., Li, Y., & Liang, Y. (2012). Decentralized kinematic control of a class of collaborative redundant manipulators via recurrent neural networks. *Neurocomputing*, *91*(2), 1–10. https://doi.org/10.1016/j.neucom.2012.01.034

Li, S., He, J., Li, Y., & Rafique, M. U. (2017). Distributed recurrent neural networks for cooperative control of manipulators: A game-theoretic perspective. *IEEE Transactions on Neural Networks and Learning Systems*, *28*(2), 415–426. https://doi.org/10.1109/TNNLS.2016.2516565

Li, S., Shao, Z., & Guan, Y. (2019). A dynamic neural network approach for efficient control of manipulators. *IEEE Transactions on Systems, Man, and Cybernetics: Systems*, *49*(5), 932–941. https://doi.org/10.1109/TSMC.6221021

Li, S., Zhang, Y., & Jin, L. (2017). Kinematic control of redundant manipulators using neural networks. *IEEE Transactions on Neural Networks and Learning Systems*,

28(10), 2243–2254. https://doi.org/10.1109/TNNLS.2016.2574363

Li, S., Zhou, M., & Luo, X. (2018). Modified primal-dual neural networks for motion control of redundant manipulators with dynamic rejection of harmonic noises. *IEEE Transactions on Neural Networks and Learning Systems*, *29*(10), 4791–4801. https://doi.org/10.1109/TNNLS.2017.2770172

Li, Z., & Huang, D. (2020). Robust control of two-link manipulator with disturbance torque and time-varying mass loads. *Transactions of the Institute of Measurement and Control*, *42*(9), 1667–1674. https://doi.org/10.1177/0142331219894413

Li, Z., Li, C., Li, S., & Cao, X. (2020). A fault-tolerant method for motion planning of industrial redundant manipulator. *IEEE Transactions on Industrial Informatics*, *16*(2), 7469–7478. https://doi.org/10.1109/TII.2019.2957186

Li, Z., Xia, Y., Wang, D., Zhai, D., Su, C., & Zhao, X. (2016). Neural network-based control of networked trilateral teleoperation with geometrically unknown constraints. *IEEE Transactions on Cybernetics*, *46*(5), 1051–1064. https://doi.org/10.1109/TCYB.2015.2422785

Li, Z., Zuo, W., & Li, S. (2020). Zeroing dynamics method for motion control of industrial upper-limb exoskeleton system with minimal potential energy modulation. *Measurement*, *163*(2), 107964. https://doi.org/10.1016/j.measurement.2020.107964

Liao, B., Zhang, Y., & Jin, L. (2016). Taylor $o(h^3)$ discretization of ZNN models for dynamic equality-constrained quadratic programming with application to manipulators. *IEEE Transactions on Neural Networks and Learning Systems*, *27*(2), 225–237. https://doi.org/10.1109/TNNLS.2015.2435014

Ma, S. (1996). A new formulation technique for local torque optimization of redundant manipulators. *IEEE Transactions on Industrial Electronics*, *43*(4), 462–468. https://doi.org/10.1109/41.510637

Maciejewski, A. A. (1991). Kinetic limitations on the use of redundancy in robotic manipulators. *IEEE Transactions on Robotics and Automation*, *7*(2), 205–210. https://doi.org/10.1109/70.75903

Su, H., Qi, W., Yang, C., Sandoval, J., Ferrigno, G., & Momi, E. D. (2020). Deep neural network approach in robot tool dynamics identification for bilateral teleoperation. *IEEE Robotics and Automation Letters*, *5*(2), 2943–2949. https://doi.org/10.1109/LSP.2016.

Su, H., Schmirander, Y., Li, Z., Zhou, X., Ferrigno, G., & De Momi, E. (2020). Bilateral teleoperation control of a redundant manipulator with an RCM kinematic constraint. In *2020 IEEE international conference on robotics and automation*. IEEE.

Su, H., Yang, C., Ferrigno, G., & De Momi, E. (2019). Improved human–robot collaborative control of redundant robot for teleoperated minimally invasive surgery. *IEEE Robotics and Automation Letters*, *4*(2), 1447–1453. https://doi.org/10.1109/LSP.2016.

Xiao, L., & Zhang, Y. (2013). Acceleration-level repetitive motion planning and its experimental verification on a six-link planar robot manipulator. *IEEE Transactions on Control Systems Technology*, *21*(3), 906–914. https://doi.org/10.1109/TCST.2012.2190142

Xu, Z., Li, S., Zhou, X., & Cheng, T. (2019). Dynamic neural networks based adaptive admittance control for redundant manipulators with model uncertainties. *Neurocomputing*, *357*(8), 271–281. https://doi.org/10.1016/j.neucom.2019.04.069

Yahya, S., Moghavvemi, M., & Mohamed, H. A. F. (2014). Artificial neural networks aided solution to the problem of geometrically bounded singularities and joint limits prevention of a three dimensional planar redundant manipulator. *Neurocomputing*, *137*(5), 34–46, advanced Intelligent Computing Theories and Methodologies. https://doi.org/10.1016/j.neucom.2013.11.038

Yang, C., Jiang, Y., He, W., Na, J., Li, Z., & Xu, B. (2018). Adaptive parameter estimation and control design for robot manipulators with finite-time convergence. *IEEE Transactions on Industrial Electronics*, *65*(10), 8112–8123. https://doi.org/10.1109/TIE.2018.2803773

Yang, C., Peng, G., Li, Y., Cui, R., Cheng, L., & Li, Z. (2019). Neural networks enhanced adaptive admittance control of optimized robot–environment interaction. *IEEE Transactions on Cybernetics*, *49*(7), 2568–2579. https://doi.org/10.1109/TCYB.6221036

Zhang, Y., Chen, S., Li, S., & Zhang, Z. (2018). Adaptive projection neural network for kinematic control of redundant manipulators with unknown physical parameters. *IEEE Transactions on Industrial Electronics*, *65*(6), 4909–4920. https://doi.org/10.1109/TIE.41

Zhang, Y., Ge, S. S., & Lee, T. H. (2004). A unified quadratic-programming-based dynamical system approach to joint torque optimization of physically constrained redundant manipulators. *IEEE Transactions on Systems, Man and Cybernetics, Part B (Cybernetics)*, *34*(5), 2126–2132. https://doi.org/10.1109/TSMCB.2004.830347

Zhang, Y., Li, S., Gui, J., & Luo, X. (2018). Velocity-level control with compliance to acceleration-level constraints: A novel scheme for manipulator redundancy resolution. *IEEE Transactions on Industrial Informatics*, *14*(3), 921–930. https://doi.org/10.1109/TII.9424

Zhang, Y., Li, S., & Zhou, X. (2019). Recurrent-neural-network-based velocity-level redundancy resolution for manipulators subject to a joint acceleration limit. *IEEE Transactions on Industrial Electronics*, *66*(5, 3573–3582. https://doi.org/10.1109/TIE.2018.2851960

Zhang, Y., Li, S., Zou, J., & Khan, A. H. (2020). A passivity-based approach for kinematic control of manipulators with constraints. *IEEE Transactions on Industrial Informatics*, *16*(5), 3029–3038. https://doi.org/10.1109/TII.9424

Zhang, Y., Wang, J., & Xia, Y. (2003). A dual neural network for redundancy resolution of kinematically redundant manipulators subject to joint limits and joint velocity limits. *IEEE Transactions on Neural Networks*, *14*(3), 658–667. https://doi.org/10.1109/TNN.2003.810607

Zhang, Z., Kong, L., Zheng, L., Zhang, P., Qu, X., Liao, B., & Yu, Z. (2020). Robustness analysis of a power-type varying-parameter recurrent neural network for solving time-varying qm and qp problems and applications. *IEEE Transactions on Systems, Man, and Cybernetics: Systems*, *50*(12), 5106–5118. https://doi.org/10.1109/TSMC.2018.2866843

Zhang, Z., Li, Z., Zhang, Y., Luo, Y., & Li, Y. (2015). Neural-dynamic-method-based dual-arm CMG scheme with time-varying constraints applied to humanoid robots. *IEEE Transactions on Neural Networks and Learning Systems*, *26*(12), 3251–3262. https://doi.org/10.1109/TNNLS.2015.2469147

Zhou, Q., Zhao, S., Li, H., Lu, R., & Wu, C. (2019). Adaptive neural network tracking control for robotic manipulators with dead zone. *IEEE Transactions on Neural Networks and Learning Systems*, *30*(12), 3611–3620. https://doi.org/10.1109/TNNLS.5962385